

# Assessment of the Microstructure and Solidification Characteristics of Al–20% Mg<sub>2</sub>Si Composite under Melt Superheating Treatment Using Thermal Analysis

Saeed G. Shabestari\*, Sahar Ashkvary, Farnaz Yavari

\* shabestari@iust.ac.ir

School of Metallurgy and Materials Engineering, Iran University of Science and Technology (IUST), Narmak, Tehran, Iran

Received: January 2021

Revised: April 2021

Accepted: July 2021

DOI: 10.22068/ijmse.2056

**Abstract:** The influence of melt superheating treatment on the solidification characteristics and microstructure of Al–20%Mg<sub>2</sub>Si in-situ composite has been investigated. The results revealed that melt superheating temperature has significant effects on solidification parameters and morphology of primary Mg<sub>2</sub>Si particles. Solidification parameters acquired using the cooling curve thermal analysis method, indicate that both nucleation temperature and nucleation undercooling of primary Mg<sub>2</sub>Si particles increase by increasing melt superheating temperature, while recalescence undercooling decrease under the same condition. Also, based on the microstructural evaluations, melt superheating treatment can refine primary Mg<sub>2</sub>Si particles and alter their morphology from dendritic shape to more spherical shape and the eutectic microstructure of  $\alpha$ -Al + Mg<sub>2</sub>Si becomes finer and the distance between eutectic layers becomes smaller.

**Keywords:** Al–20%Mg<sub>2</sub>Si in-situ composite; melt superheating treatment; cooling curve thermal analysis; microstructure; solidification

## 1. INTRODUCTION

Al–Mg<sub>2</sub>Si metal matrix composites (MMCs) have the potential to replace the commonly used hypereutectic Al–Si alloys due to their improved properties (low density, excellent castability, good wear resistance, and excellent mechanical properties) [1, 2]. The characteristics of Mg<sub>2</sub>Si intermetallic compound as reinforcing particles play a major role in superior mechanical properties of this material, which includes low density (1.99 g.cm<sup>-3</sup>), high melting temperature (1085°C), high hardness ( $4.5 \times 10^9$  N.m<sup>-2</sup>), high elastic modulus (120 GPa) and low coefficient of thermal expansion ( $7.5 \times 10^{-6}$  K<sup>-1</sup>) [2-6]. According to Al–Mg<sub>2</sub>Si binary phase diagram, Al–Mg<sub>2</sub>Si composite containing more than 13.9 wt. % Mg<sub>2</sub>Si demonstrates a hypereutectic microstructure [7]. The first phase precipitating from the melt is primary Mg<sub>2</sub>Si, and then the rest of the melt solidifies as a binary eutectic structure consisting of Al and Mg<sub>2</sub>Si [2, 7]. Mechanical properties of hypereutectic Al–Mg<sub>2</sub>Si highly depend on the morphology and size of primary Mg<sub>2</sub>Si. In as-cast conditions, primary Mg<sub>2</sub>Si has coarse dendritic morphology with sharp edges and needs to be modified to improve mechanical properties [3]. The most popular refinement method is adding a refiner element to the melt. It

has been reported that the addition of Bi [8, 9], Sr [3, 9, 10], Sb [9, 11, 12], Mn [13], P [10], and Ce [2] can change coarse dendritic structure of Mg<sub>2</sub>Si particles to fine polygonal shapes.

Melt superheating treatment has been reported as an effective technique for Mg<sub>2</sub>Si refinement in a few Al and Mg alloys and composites [14-18]. In general, there are two main hypotheses for the grain refining effect of melt superheating treatment. The first theory is called the ‘heredity phenomenon’. Based on this theory existing particles in the melt at normal pouring temperatures are too big to serve as nucleation sites. Higher superheating temperatures dissolve these particles and then they precipitate as finer more suitable nuclei [16, 18]. Z. H. Gu et.al [15] reported that reduction of heredity plays an important role in the grain refinement of Mg–1.5Si–1Zn alloy. In the second theory, an increase in undercooling is the reason for the grain refining effect of melt superheating treatment. It means by increasing superheating temperature the distribution of alloying elements will be more homogeneous due to the thermal diffusion which clearly affects the undercooling and the subsequent solidification process [18].

This paper aims to study the effect of melt superheating treatment on microstructure and solidification parameters of Al-20wt% Mg<sub>2</sub>Si

composite. For this purpose, the cooling curve thermal analysis (CCTA) technique has been used along with microstructural evaluations. Backerud et al. [19, 20] and S.G. Shabestari et al. [21-24] have used CCTA as a very useful method to investigate the relationship between solidification characteristics and microstructure of different metals and alloys. To date, only a few numbers of research [14] have reported about the investigation on the effect of melt superheating on nucleation and growth of  $Mg_2Si$  reinforcement at in-situ composite through thermal analysis, but there is no report on other solidification aspects of this composite. In the present study characteristic temperatures including nucleation and growth temperatures ( $T_N$ ,  $T_G$ ) and nucleation and recalescence undercooling ( $\Delta T_N$ ,  $\Delta T_R$ ) for different phases are determined from cooling curves and their first derivative at different melt superheating temperatures. Also, the relation between solidification parameters and microstructure is studied.

## 2. EXPERIMENTAL PROCEDURES

The Al-20Mg<sub>2</sub>Si composite was prepared by melting commercially A413 alloy and high purity (>99.99 wt %) magnesium in a graphite crucible in an electrical resistance furnace. The melt was protected with Magrex\* powder as a coveral flux to prevent melt oxidation and gas absorption. (\* It is the trademark of Foseco company.) The melt was held for 10 min at  $750 \pm 5^\circ C$  for homogenization, then it was skimmed and poured into a steel permanent mold coated with graphite and preheated to  $250^\circ C$  to produce Al-20%Mg<sub>2</sub>Si ingot. The chemical composition of the investigated composite is listed in table 1.

**Table 1.** Chemical composition of prepared Al-Mg<sub>2</sub>Si composite

| Composite                  | Elements (mass %) |      |      |      |         |
|----------------------------|-------------------|------|------|------|---------|
|                            | Mg                | Si   | Cu   | Fe   | Al      |
| Al – 20%Mg <sub>2</sub> Si | 13.93             | 9.63 | 0.12 | 0.32 | Balance |

Thermal analysis samples were taken by remelting 200 g of prepared ingot in a graphite crucible and pouring the molten alloy into a preheated cylindrical stainless steel mold (outer diameter 40 mm, height 70 mm, and wall thickness of 1 mm) which a K-type thermocouple had been placed in the center of it at a position of

20 mm from the bottom. To study the influence of superheating, the melt was held at 750, 800, and  $850^\circ C$  for 25 min. before pouring. The temperature-time data were recorded using an analog to digital converter (A/D converter) linked to a computer. The analog to digital converter ADAM- 4018 used in this study has a sensitive 16-bit microprocessor-controlled sigma-delta A/D converter; the response time of 0.02 seconds and having 8-channel analog input module that provides programmable input ranges on all channels. Each test was repeated at least three times, to check the reproducibility and accuracy. The variations of temperature versus time were recorded with the frequency of 10 readings per second. Solidification parameters have been extracted from cooling curves and their first derivative. The cooling rate (C.R) during thermal analysis tests was  $0.50 \pm 0.05^\circ C s^{-1}$  which was calculated from the slope of the cooling curve,  $\Delta T/\Delta t$ , between the two first reactions ( $670^\circ C$  to  $620^\circ C$ ).

For microstructural evaluations, samples were sectioned horizontally from the regions near the thermocouple tip. After grinding and polishing the samples, they were etched using 0.5% HF etchant to reveal as-cast microstructure of samples. The morphology and size of primary Mg<sub>2</sub>Si particles were analyzed using HUVITZ – HM25 type optical microscope. For each sample, five pictures were taken from the central zone and Mg<sub>2</sub>Si particles size, circularity, and aspect ratio were evaluated for each picture using Image J software. Then, the average particle size, circularity, and aspect ratio of primary Mg<sub>2</sub>Si intermetallics were determined in each sample. The phases were also characterized through X-ray diffraction XRD D8 Advance Bruker using Xpert High Score software.

## 3. RESULTS AND DISCUSSION

### 3.1. Al-Mg<sub>2</sub>Si in situ composite; cooling curve and microstructure

The cooling curve and its first derivative curve for Al-20%Mg<sub>2</sub>Si composite with melt superheating temperature of  $800^\circ C$  are given in Fig 1-a. The derivative curve is projected to reveal the characteristic data, such as nucleation, growth, and minimum temperatures ( $T_N$ ,  $T_G$ , and  $T_{min}$ ) because these temperatures cannot be identified easily from the cooling curve itself. Three slope

alterations on the cooling curve and three well-known peaks on the first derivative curve are noticeable which correspond to three-phase transformations or phase formation during the solidification. These phases are shown in Fig 1-b.

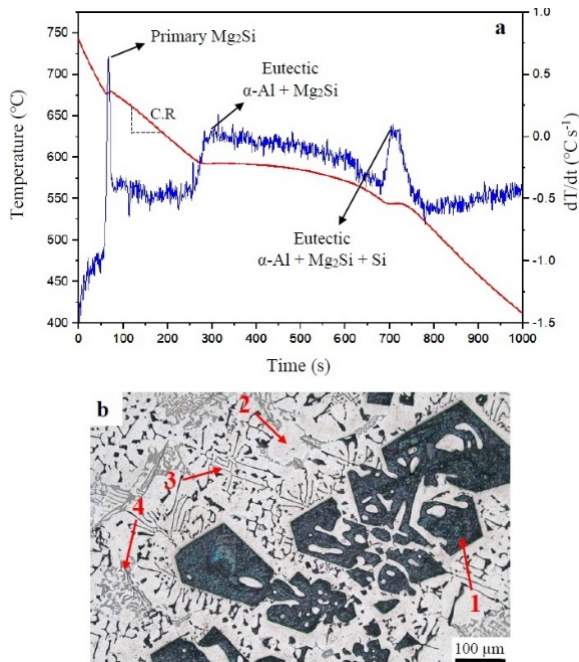


**Fig. 1.** (a) cooling curve and its first derivative curve (b) microstructure of Al-20% Mg<sub>2</sub>Si in situ composite with 800°C superheating temperature indicated phases: (1) primary Mg<sub>2</sub>Si, (2) α-Al, (3) eutectic Mg<sub>2</sub>Si, (4) eutectic Si

According to Al-Mg<sub>2</sub>Si binary phase diagram [1] (Fig.2), solidification of Al-20%Mg<sub>2</sub>Si starts with nucleation of primary Mg<sub>2</sub>Si.

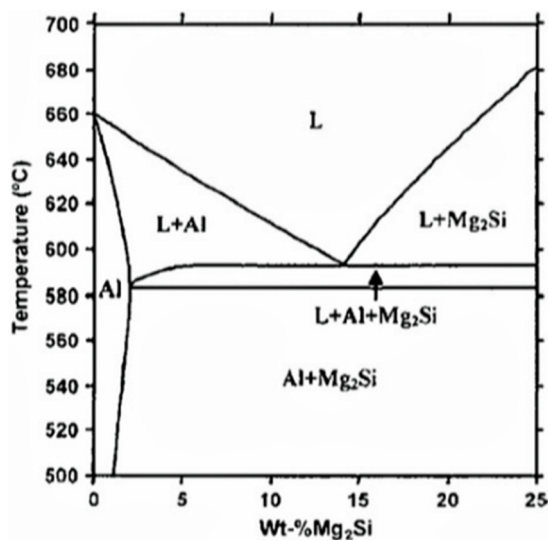


**Fig. 2.** Al-Mg<sub>2</sub>Si binary phase diagram [1]

Therefore, the first peak at 687°C relates to the formation of primary Mg<sub>2</sub>Si. The second peak at 600°C and the third peak at 547°C represent binary α-Al + Mg<sub>2</sub>Si eutectic and ternary α-Al + Mg<sub>2</sub>Si + Si eutectic, respectively. The phases were also analyzed with XRD. They were characterized as α-Al and Mg<sub>2</sub>Si phases in the microstructure of the composite (Fig.3). Because of the low concentration of the Si phase, this phase wasn't recognized in the XRD pattern.

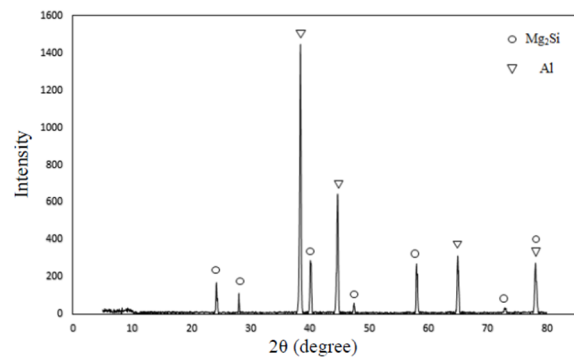


**Fig. 3.** XRD pattern of as-cast Al-20%Mg<sub>2</sub>Si in situ composite

### 3.2. Effect of melt superheating treatment on cooling curves

The cooling curve of Al-20%Mg<sub>2</sub>Si composite with different superheating temperatures is illustrated in Fig 4. Characteristic temperatures for each reaction are extracted from cooling curves and their derivative curves as it is shown in Fig 5 and presented in Table 2. Thermal analysis results in Table 2 reveal that superheating treatment has significant effects on nucleation of primary Mg<sub>2</sub>Si particles and binary α-Al + Mg<sub>2</sub>Si eutectic.

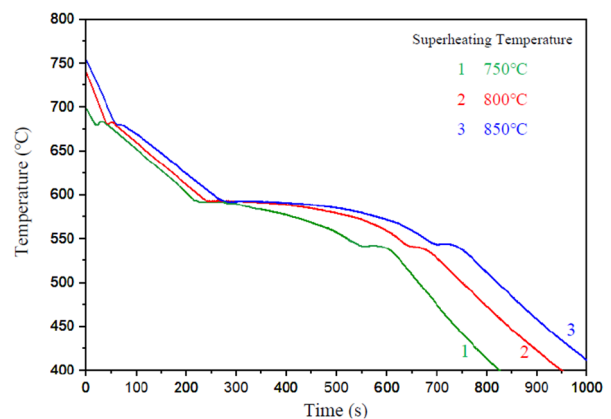


**Fig. 4.** Effect of superheating temperature on cooling curves

**Table 2.** Characteristic temperatures determined from cooling curves and their first derivative curves

| Superheating Temperature (°C) | Primary Mg <sub>2</sub> Si |                |                  |                 |                 | Eutectic α-Al + Mg <sub>2</sub> Si |                | Eutectic α-Al + Mg <sub>2</sub> Si + Si |                | Solidus temperature (T <sub>s</sub> ) |
|-------------------------------|----------------------------|----------------|------------------|-----------------|-----------------|------------------------------------|----------------|---|----------------|---------------------------------------|
|                               | T <sub>N</sub>             | T <sub>G</sub> | T <sub>Min</sub> | ΔT <sub>N</sub> | ΔT <sub>R</sub> | T <sub>N</sub>                     | T <sub>G</sub> | T <sub>N</sub>                          | T <sub>G</sub> |                                       |
| 750                           | 686.0                      | 683.2          | 678.5            | 7.5             | 4.7             | 599.3                              | 593.7          | 547.2                                   | 540.5          | 527.2                                 |
| 800                           | 687.5                      | 679.8          | 676.5            | 11.0            | 3.3             | 601.7                              | 592.6          | 546.9                                   | 540.7          | 522.5                                 |
| 850                           | 690.3                      | 677.2          | 676.2            | 14.1            | 1.0             | 602.4                              | 589.5          | 547.4                                   | 541.1          | 519.9                                 |

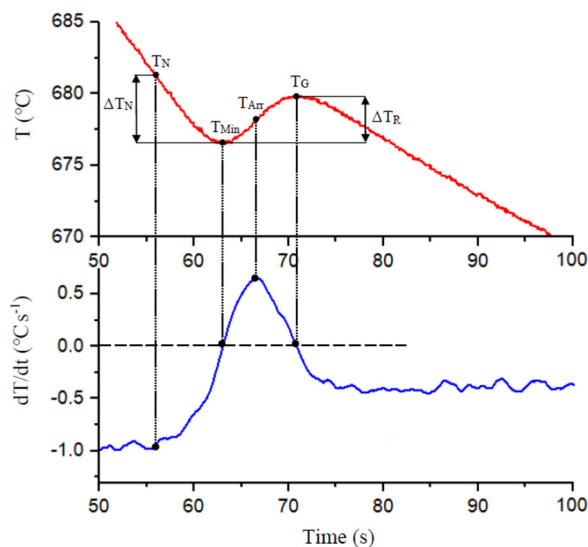


**Fig. 5.** Characteristic points on cooling curve and its first derivative

### 3.2.1. Effect of superheating on the nucleation of primary Mg<sub>2</sub>Si

Variation of nucleation temperature (T<sub>N</sub>), nucleation undercooling (ΔT<sub>N</sub> = T<sub>N</sub> - T<sub>Min</sub>), and recalescence undercooling (ΔT<sub>R</sub> = T<sub>G</sub> - T<sub>Min</sub>) for primary Mg<sub>2</sub>Si particles illustrated in Fig 6. According to this figure, by increasing superheating temperature from 750 °C to 850 °C, T<sub>N</sub> and ΔT<sub>N</sub> increase from 686.0 °C to 690.3 °C, and 7.5 °C to 14.1 °C, respectively; but ΔT<sub>R</sub> decreases from 4.7 °C to 1.0 °C.

Increasing the nucleation temperature of Mg<sub>2</sub>Si may be a result of the acceleration of atomic diffusion in the melt by increasing the superheating temperature which provides more potential substrates for Mg<sub>2</sub>Si particles to nucleate. Therefore, primary Mg<sub>2</sub>Si particles are expected to become finer by melt superheating treatment. In the other hand, with increasing superheating temperature, existing impurities and atomic clusters in the melt decrease. As a result of the reduction in the number of heterogeneous nucleation sites and because the new atomic

clusters have a smaller radius than the critical radius of the nuclei, nucleation undercooling of primary Mg<sub>2</sub>Si increases.

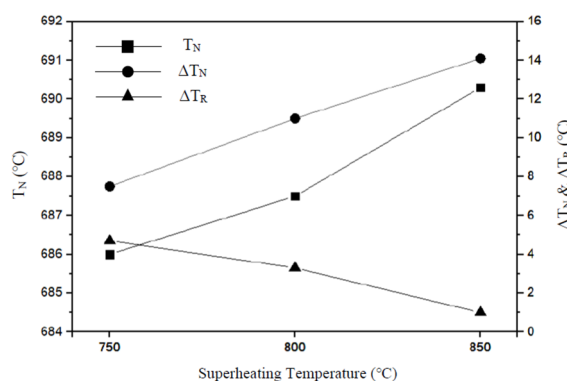


**Fig. 6.** Effect of superheating temperatures on nucleation temperature (T<sub>N</sub>), nucleation undercooling (ΔT<sub>N</sub>) and recalescence undercooling (ΔT<sub>R</sub>) for primary Mg<sub>2</sub>Si particles

Backerud et al. [19] and Shabestari et al. [24] reported that grain refinement in different Al alloys causes to decline of recalescence undercooling until there would be no recalescence undercooling (ΔT<sub>R</sub> = 0) when the optimum amount of refiner is added. In the present work, the reduction of ΔT<sub>R</sub> can be another sign for the refinement of primary Mg<sub>2</sub>Si particles, too. In Table 2 and Fig. 6, the effect of melt superheating on the recalescence undercooling has been presented. As can be seen, the recalescence undercooling has been decreased by increasing superheating temperature. The reason for this phenomenon is that with increasing superheating temperature, existing nuclei in the melt can become more active because of the higher diffusion rate that happens at higher superheating temperatures and can establish the condition of the growth. In this situation, it can achieve the growth temperature with lower recalescence undercooling. Therefore, a decrease in recalescence undercooling can cause the

refinement of primary  $Mg_2Si$ .

In addition, solid fraction curves were plotted based on the Newtonian model adopted by Stefanescu et al. and Tamminen [25] and shown in Fig. 7. According to this figure, when superheating temperature increase from  $750^\circ C$  to  $850^\circ C$ , the solid fraction between the two first reactions (nucleation of primary  $Mg_2Si$  and binary  $\alpha-Al + Mg_2Si$  eutectic) increases significantly.

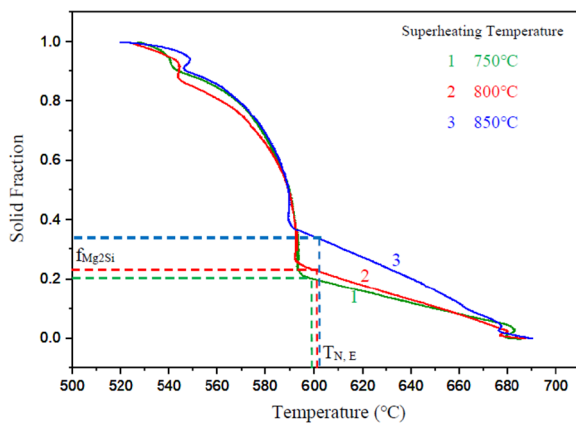


Fig. 7. Effect of superheating temperature on solid fraction curves

Solid fraction of primary  $Mg_2Si$  (solid fraction at nucleation temperature of binary eutectic) was extracted from Fig.7. By increasing superheating temperature, the solid fraction of primary  $Mg_2Si$  increases from 0.20 to 0.33. It means the fraction of eutectic  $Mg_2Si$  has decreased since the amount of Mg and Si in the composition of samples are constant.

### 3.2.2. Effect of superheating on the final solidification temperature, solidification range, and total solidification time

Fig. 8 shows the effect of superheating on the final solidification temperature, solidification range, and total solidification time. As seen from this figure, with increasing superheating temperature, the final solidification temperature decreases, while the solidification range, and total solidification time increase.

In section 3.2.1, it has been reported that the nucleation temperature of primary  $Mg_2Si$  increases with superheating. In Fig. 8, it is shown that the final solidification temperature decreases with superheating. Therefore, the solidification range which is the difference between these two parameters will increase with superheating temperature.

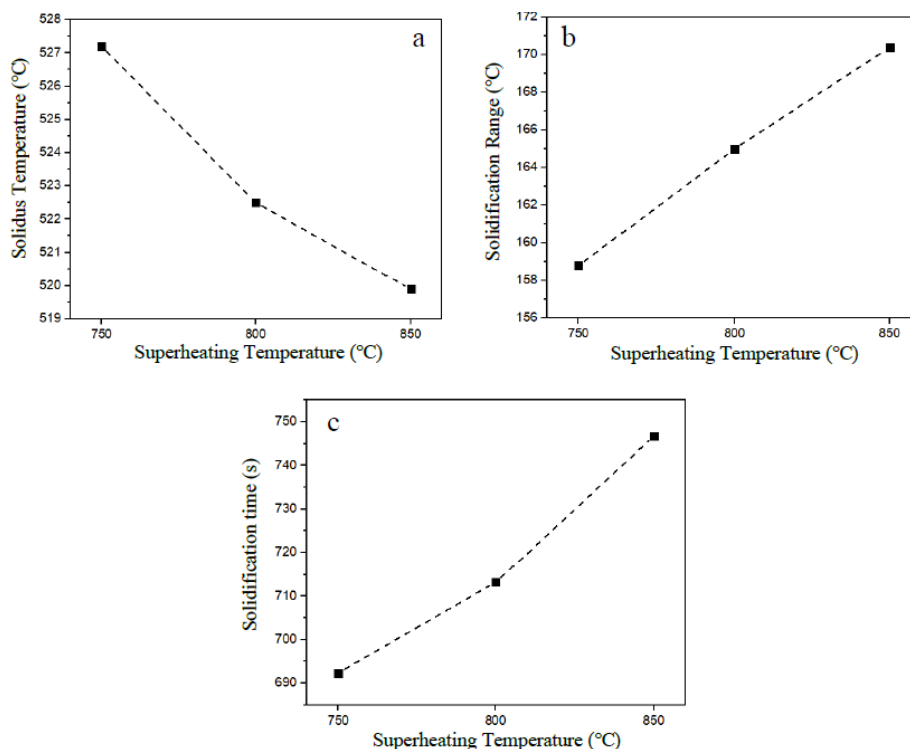
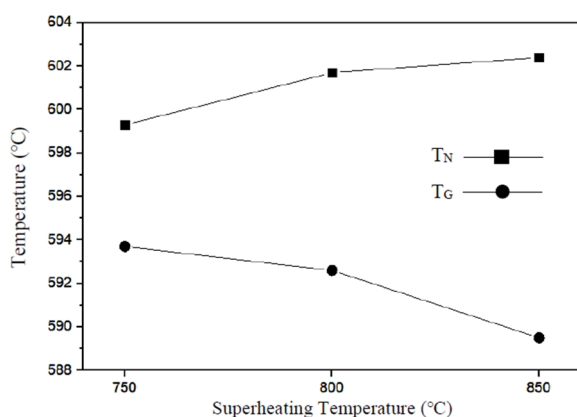


Fig. 8. Effect of superheating on: (a) the final solidification temperature, (b) solidification range, (c) total solidification time.

### 3.2.3. Effect of superheating on the eutectic reactions

Fig. 9 indicates the effect of superheating on the binary eutectic reaction of  $\alpha$ -Al +  $Mg_2Si$ . It can be observed that with increasing superheating temperature, nucleation temperature of the binary eutectic reaction increases and the growth temperature decreases. It has been proved that primary  $Mg_2Si$  particles act as heterogeneous sites for the nucleation of eutectic  $\alpha$ -Al [26, 27].



**Fig. 9.** Effect of superheating on nucleation and growth temperatures of  $\alpha$ -Al +  $Mg_2Si$  eutectic reaction

In section 3.2.1, it has been explained that primary  $Mg_2Si$  particles will be finer and their volume fraction increase by increasing superheating temperature. Therefore, there are more suitable sites for nucleation of eutectic  $\alpha$ -Al and it can be the reason for the increase in nucleation temperature of the binary eutectic reaction. On the other hand, because of the higher volume fraction of primary  $Mg_2Si$ , the concentration of Si and Mg in the melt would be lower and it probably reduces the growth temperature of this eutectic reaction.

Results of cooling curves obtained from applying melt superheating temperatures of 750°C, 800°C, 850°C indicate that they do not have any effect on ternary eutectics.

### 3.3. Effect of melt superheating treatment on microstructure

#### 3.3.1. Effect of superheating on primary $Mg_2Si$

Fig. 10 shows the changes of morphology and size of primary  $Mg_2Si$  particulate in Al-20%  $Mg_2Si$  in situ composite as a result of various superheating temperatures.

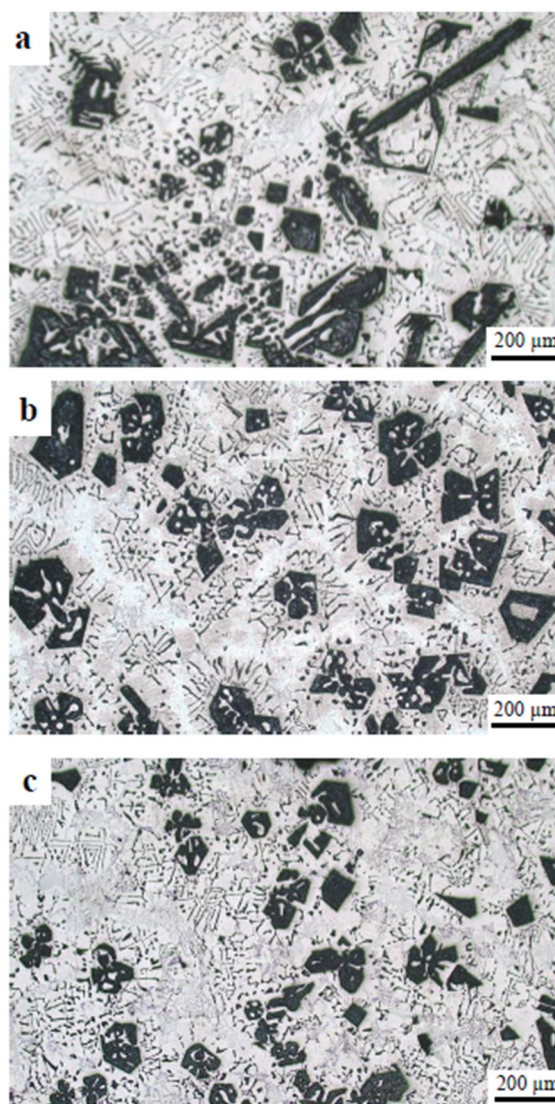


**Fig. 10.** Primary  $Mg_2Si$  microstructure of Al-20%  $Mg_2Si$  composite by applying melts superheating, (a) 750°C, (b) 800°C, (c) 850°C

Obviously, higher melt superheating temperature leads to better refinement of primary  $Mg_2Si$  particles. Microstructural analysis indicates that by increasing superheating temperature from 750°C to 850°C,  $Mg_2Si$  particles size decrease from 134.5  $\mu m$  to 113.3  $\mu m$  (Fig. 11). This is in good agreement with thermal analysis results. Reduction of heredity of the molten composite by melt superheating treatment can explain this phenomenon [14-16]. It means that all solid particles and impurities would dissolve completely in higher superheat temperatures and re-nucleate as finer particles. Since these particles might be responsible for primary  $Mg_2Si$  precipitation, finer particles lead to finer  $Mg_2Si$  particles. Also, an increase in nucleation

undercooling and a decrease in recalescence undercooling, which has been discussed in section 3.2.1, is another explanation for the refinement of primary  $Mg_2Si$  particles.

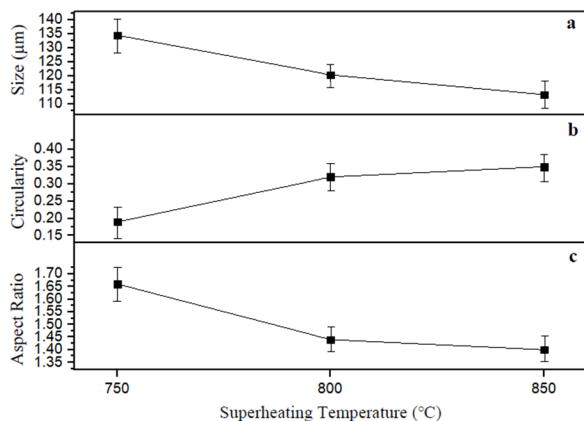


**Fig. 11.** Variation of (a) size, (b) circularity and (c) aspect ratio of primary  $Mg_2Si$  particles versus melt superheating temperature

In addition to the reduction of  $Mg_2Si$  particles size, the dendritic shape of the particles has changed to a more spherical shape. The influence of superheating temperature on aspect ratio and circularity of primary  $Mg_2Si$  particles are shown in Fig. 11. The aspect ratio defines as the ratio of the maximum length to the minimum length of the primary  $Mg_2Si$  particle.

It can be seen that the aspect ratio decreases from 1.66 to 1.40 when superheating temperature changes from 750°C to 850°C; while circularity increase from 0.19 to 0.35 at the same condition. In another word, superheating treatment is caused primary  $Mg_2Si$  particles to become more spherical and finer.

### 3.3.2. Effect of superheating on eutectic microstructure

Fig. 12 indicates the effect of superheating on the eutectic microstructure of Al-20%  $Mg_2Si$  composite. The morphology of the  $\alpha$ -Al +  $Mg_2Si$  eutectic does not change; but the eutectic microstructure becomes finer and the distance between eutectic layers becomes smaller.

## 4. CONCLUSION

Effect of various melt superheating temperatures (750, 800, and 850°C) on Al-20% $Mg_2Si$  in-situ composite was investigated through thermal analysis technique. Microstructure and

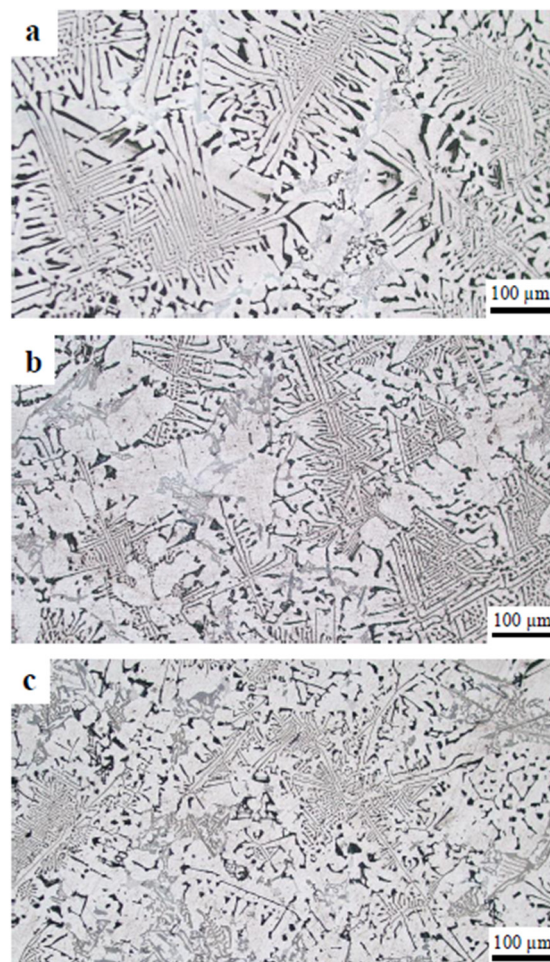


**Fig. 12.** Eutectic microstructure of Al-20% $Mg_2Si$  composite by applying melts superheating, (a) 750°C, (b) 800°C, (c) 850°C

solidification parameters of the composite were studied using cooling curves. Nucleation and growth of  $Mg_2Si$  intermetallic as reinforcement phase at in-situ composite was studied.

Microstructural analysis indicated that by increasing superheating temperature from 750°C to 850°C,  $Mg_2Si$  particles size decrease from 134.5  $\mu m$  to 113.3  $\mu m$ , and the dendritic shape of the particles has changed to a more spherical shape. Also, the eutectic microstructure of  $\alpha$ -Al +  $Mg_2Si$  becomes finer and the distance between eutectic layers becomes smaller.

When melt superheating temperature was 850°C, primary  $Mg_2Si$  particles had the highest nucleation temperature (TN) and the lowest recalescence undercooling ( $\Delta TR$ ). These two parameters are known as the main sign of grain refinement in various alloys. Since microstructural evaluations revealed that increasing superheating temperature leads to finer

and more spherical primary  $Mg_2Si$  particles, TN and  $\Delta TR$  can be used as the sign of  $Mg_2Si$  particles refinement in Al- $Mg_2Si$  composites. Therefore, the cooling curve thermal analysis technique can be used as an online method to control the refinement of  $Mg_2Si$  reinforcement particles during the casting process of Al- $Mg_2Si$  composites.

## 5. REFERENCES

- [1] Emamy, M, Tavighi, K and Pourbahari, B, "Improvement in tensile and wear properties of as-cast Al-15% $Mg_2Si$  composite modified by Zn and Ni" *Int. J. Met. Cast.*, 2017, 11, 790–801.
- [2] Li, C, Wu, Y. Y, Li, H and Liu, X. F, "Morphological evolution and growth mechanism of primary  $Mg_2Si$  phase in Al- $Mg_2Si$  alloys" *Acta. Mater.*, 2011, 59, 1058–1067.
- [3] Farahany, S, Ghandvar, H, Bozorg, M, Nordin, A, Ourdjini, A and Hamzah, E, "Role of Sr on microstructure, mechanical properties, wear and corrosion behaviour of an Al- $Mg_2Si$ -Cu in-situ composite" *Mater. Chemist. Physics*, 2020, 239, 121954.
- [4] Nordin, N. A, Farahany, S, Abubakar, T, Hamzah, E and Ourdjini, A, "Microstructure development, phase reaction characteristics and mechanical properties of a commercial Al-20% $Mg_2Si$ -xCe in-situ composite solidified at a slow cooling rate" *J. Alloy. Compd.*, 2015, 650, 821 – 834.
- [5] Li, CH, Wu, Y, Li, H and Liu, X, "Microstructural formation in hypereutectic Al- $Mg_2Si$  with extra Si" *J. Alloys. Compounds.*, 2009, 477, 212–216.
- [6] Shabestari, S. G, Saghafian, H, Sahihi, F and Ghoncheh, M. H, "Investigation on microstructure of Al-25 wt-% $Mg_2Si$  composite produced by slope casting and semi-solid forming" *Int. J. Cast Met. Res.*, 2015, 28, 158-166.
- [7] Zhang, J, Fan, Z, Wang, Y. Q and Zhou, B. L, "Equilibrium pseudobinary Al –  $Mg_2Si$  phase diagram" *Mater. Sci. Technol.*, 2001, 17, 494-496.
- [8] Guo, E.J, Ma, B.X and Wang, L.P, "Modification of  $Mg_2Si$  Morphology in Mg-Si Alloys with Bi" *J. Mater. Process. Technol.*, 2008, 206, 161-166.
- [9] Nordin, N. A, Farahany, S, Ourdjini, A, AbuBakar, T and Hamzah, E, "Refinement of  $Mg_2Si$  reinforcement in a commercial Al-20% $Mg_2Si$  in-situ composite with bismuth, antimony and strontium" *Mater. Charact.*, 2013, 83, 97–107.
- [10] Tebib, M, Samuel, A.M, Ajersch, F and Chen, X.-G, "Effect of P and Sr additions on the microstructure of hypereutectic Al-15Si-14Mg-4Cu alloy" *Mater. Charact.*, 2014, 89, 112–123.
- [11] Bo, R, Zhong-xia, L, Rui-feng, Z, Tian-qing Z, Zhi-yong, L, Ming-xing, W and Yong-gang, W, "Effect of Sb on microstructure and mechanical properties of  $Mg_2Si$ /Al-Si composites" *Trans. Nonferrous Met. Soc. China*, 2010, 20, 1367–1373.
- [12] Yu-hua Zhao, Xiu-bin Wang, Xing-hao Du and Chao Wang, "Effects of Sb and heat treatment on the microstructure of Al-15.5wt%  $Mg_2Si$  alloy" *Int. J. Min. Metall. Mater.*, 2013, 20, 653-658.
- [13] Ghorbani, M.R, Emamy, M, Khorshidi, R, Rasizadehghania, J and Emami, A.R, "Effect of Mn addition on the microstructure and tensile properties of Al-15% $Mg_2Si$  composite" *Mater. Sci. Eng. A*, 2012, 550, 191– 198.
- [14] Nordin, N. A, Abubakar, T, Hamzah, E, Farahany, S and Ourdjini, A, "Effect of superheating melt treatment on  $Mg_2Si$  particulate reinforced in Al- $Mg_2Si$ -Cu in-situ composite" *Procedia Eng.*, 2017, 184, 595 – 603.
- [15] Gu, Z. H, Wang, H. Y, Zheng, N, Zha, M, Jiang, L. L, Wang, W and Jiang, Q. C, "Effect of melt superheating treatment on the cast microstructure of Mg-1.5Si-1Zn alloy" *J. Mater. Sci.*, 2008, 43, 980–984.
- [16] Zha, M, Wang, H. Y, Liu, B, Zhao, B, Liang, M. L, Li, D and Jiang, Q. C, "Influence of melt superheating on microstructures of Mg-3.5Si-1Al alloys" *Trans. Nonferrous Met. Soc. China*, 2008, 18, 107–112.
- [17] Liu, Z, Xie, M and Liu, X. M, "Microstructure and properties of in-situ Al-Si- $Mg_2Si$  composite prepared by melt superheating" *Appl. Mech. Mater.*, 2011,



- 52, 750-754.
- [18] Qin, Q.D, Zhao, Y.G, Y.H. Liang, Y.H and Zhou, W, "Effects of melt superheating treatment on microstructure of Mg<sub>2</sub>Si/Al-Si-Cu composite" *J. Alloy. Compd.*, 2005, 399, 106-109.
- [19] Backerud, L, Chai, G and Tamminen, J, *Solidification characteristics of aluminum alloys, Vol. 2: Foundry Alloys*, Skan Aluminum, Stockholm-Sweden, 1990.
- [20] Backerud, L, and Sigworth, G.K, "Recent development in thermal analysis of aluminum casting alloys" *AFS Trans.*, 1989, 97, 459-64.
- [21] Shabestari, S.G, Ghoncheh, M.H and Momeni, H, "Evaluation of formation of intermetallic compounds in Al2024 alloy using thermal analysis technique" *Thermochim. Acta.*, 2014, 589, 174-182.
- [22] Shabestari, S.G and Malekan, M, "Thermal analysis study of the effect of the cooling rate on the microstructure and solidification parameters of 319 aluminum alloy" *Canadian. Metall. Quar.*, 2005, 44, 305-312.
- [23] Yavari, F and Shabestari, S.G, "Effect of cooling rate and Al content on solidification characteristics of AZ magnesium alloys using cooling curve thermal analysis" *J. Therm. Analys. Cal.*, 2017, 129, 655-662.
- [24] Shabestari, S.G and Malekan, M, "Assessment of the effect of grain refinement on the solidification characteristics of 319 aluminum alloy using thermal analysis" *J. Alloy. Compd.*, 2010, 492, 134-142.
- [25] Backerud, L, Krol, E, and Tamminen, J, *Solidification Characteristics of Aluminum Alloys. Vol. 1: Wrought Aluminum Alloys*, Skan Aluminum, Sweden, 1986.
- [26] Zhang, J, Fan, Z, Wang, Y.Q and Zhou, B.L, "Microstructural development of Al-15wt%Mg<sub>2</sub>Si in situ composite with mischmetal addition" *Mater. Sci. Eng. A*, 2000, 281, 104-112.
- [27] Nasiri, N, Emamy, M, Malekan, A and Norouzi, M.H, "Microstructure and tensile properties of cast Al-15%Mg<sub>2</sub>Si composite: Effects of phosphorous addition and heat treatment" *Mater. Sci. Eng. A*, 2012, 556, 446-453.